Petratherm Limited
Level 1, 129 Greenhill Road, Unley, South Australia 5061
e: admin@petratherm.com.au ASX: PTR
A.BN. 17 106 806 884

GEP-24

Petratherm Limited

Geothermal Data Submission

09/2009

Author: Mathieu Messeiller

Date: 23rd of September 2009

Table of Contents

1. Thermal conductivity measurements 3

1.1 Introduction 3

1.2 Methodology 3

1.3 Results 4

1.4 Discussion and conclusions 5

2. Temperature logging operation and heat flow model 6

2.1 Introduction 6

2.2 Heat flow 6

2.3 Results 7

3. Core analysis 7

3.1 Introduction 7

3.2 Methodology 8

3.2.1 Sample preparation 8

3.2.2 Cleaning and drying 8

3.2.3 Porosity 8

3.2.4 Permeability to air 9

3.2.5 Grain density 9

3.3 Results 9

4. Petrographic description 9

4.1 Introduction 9

4.2 Methodology 10

4.3 Petrographic description 10

4.3.1 Hand specimen 10

4.3.2 Rock name 10

4.3.3 Petrography 10

4.3.4 Interpretation 11

1. Introduction

In accordance with the Regulations requirements, Petratherm Ltd submits in the present report and accompanying digital data the geothermal data collected in relation to the tenement GEP24 for the period comprised between the 31st of March 2009 and the 31st of August 2009. A list of the contractors commissioned for each data collection is available in Appendix 1. A CD containing the digital data is enclosed with the present report.

2. Thermal conductivity measurements

2.1 Introduction

Thermal conductivity is the physical property that controls the rate at which heat energy flows through a material in a given thermal gradient. In the S.I. system of units, it is measured in watts per metre-Kelvin (W/mK). In the Earth, thermal conductivity controls the rate at which temperature increases with depth for a given heat flow. The thermal conductivity distribution within a section of crust must be known in order to calculate crustal heat flow from temperature gradient data, or to predict temperature distribution from a given heat flow. This section describes the results of laboratory thermal conductivity measurements on a series of drill core samples. Petratherm commissioned Hot Dry Rocks Pty Ltd (HDRPL) to undertake this study. HDRPL took delivery of 8 core specimens in April 2009 from two onshore Gippsland Basin wells, Wellington Park 1 and Dutson Downs 1 and collected 8 samples from the well Sale 13 in July 2009. Thermal conductivity and density measurements were made on all specimens using a steady state divided bar apparatus calibrated for the range 1.4–9.8 W/mK. Thermal conductivity is sensitive to temperature, in general decreasing as temperature increases. The measurements contained in this report were made within ± 2°C of 25°C.

2.2 Methodology

HDRPL received 8 specimens of consolidated core from PTR and collected 8 samples on the behalf of PTR. HDRPL assumed that the specimens were representative of the average lithological composition of the formation being sampled.

Each specimen was prepared for thermal conductivity measurement in a divided bar apparatus. Three prisms were cut from each consolidated core, each approximately ⅓ to ½ the width of the specimen in thickness. These samples were taken to investigate variation in thermal conductivity over short distance scales and to determine mean conductivity and uncertainty. The samples were generally of a quarter-core shape. Each sample was ground flat and polished, then evacuated under >95% vacuum for a minimum of three hours. Samples were then submerged in water prior to returning to atmospheric pressure. Water saturation continued at atmospheric pressure for a minimum of three hours, and all samples were left in water until just prior to conductivity measurement. Specimens PTR008, PTR009, PTR011, PTR013, PTR015, and sample PTR014C, being friable, were prepared via the use of a hollow cell. Uncertainties of thermal conductivity associated with this preparation method are ± 15%. Values were measured at a standard temperature of 25°C (± 2°C). Harmonic mean conductivity and one standard deviation uncertainty were calculated for each specimen.

2.3 Results

Table 1 displays the thermal conductivity for each individual sample, and the harmonic mean conductivity and standard deviation for each specimen. All values are for a standard temperature of 25°C. The uncertainty for individual is approximately ± 3.5% for consolidated samples (based on the instrument precision of the divided bar apparatus). For samples prepared via the hollow cell method, uncertainties are within ± 10%.

Sample ID	Well	from (m)	to (m)	Sample Conductivity (W/mK)	uncertainty	lithology	description
PTRGPL1	Wellington Park 1	1320.8	1321.1	2.17	0.09	Greywacke	Grey, finely bedded, fine to medium grained GRWK, rich in carb frag, sly micaceous, steep calcite veining
PTRGPL2	Wellington Park 1	1775.8	1776	2.41	0.07	Greywacke	Green-grey medium grained GRWK, chloritic matrix, rare coal fragments
PTRGPL3	Wellington Park 1	2085.8	2086	1.97	0.07	Silstone	Dark grey-brown, finely laminated siltstone, fractured, slightly micaceous
PTRGPL4	Wellington Park 1	3211.4	3211.5	2.22	0.1	Silstone	Dark grey-green siltstone and shale, finely laminated, slumps
PTRGPL5	Dutson Downs 1	1859	1859.1	3.04	0.09	Mudstone	Grey mudstone sly micaceous, associated with interbedded medium to coarse sandstone
PTRGPL6	Dutson Downs 1	1859.8	1859.9	2.78	0.02	Arkose	Light grey medium to coarse arkose, incorporating mudstone clast, coal-rich horizons
PTRGPL7	Dutson Downs 1	551.8	552	1.81	0.07	Marly limestone	Grey-orange argillaceous limestone
PTRGPL8	Dutson Downs 1	553.8	554.1	1.11	0.03	Marl	Brown-yellow fossiliferous marl
PTRGPL9	Sale 13	127.5	127.8	1.82	0.11	Marl	Pale grey marl/fine sand, fossiliferous, micaceous, calcareous
PTRGPL10	Sale 13	170.4	170.8	1.45	0.07	Marl	Pale grey marl, fossiliferous, micaceous, calcareous
PTRGPL11	Sale 13	266.55	266.75	1.21	0.03	Marl	Pale grey consolidated fossiliferous marl, calcareous
PTRGPL12	Sale 13	564.45	564.7	2.35	0.08	Limstone	Pale grey fossiliferous limestone, hard
PTRGPL13	Sale 13	746.1	746.4	1.54	0.12	Mudstone	Pale grey calcareous mudstone to sandstone
PTRGPL14	Sale 13	841.5	841.7	0.49	0.02	Coal	Brown coal, core
PTRGPL14	Sale 13	842	843	0.49	0.02	Coal	Brown coal, chips
PTRGPL15	Sale 14	870	871	0.5	0.04	Coal	Brown coal and carbonaceous mudstone
PTRGPL16	Sale 13	910	910.4	1.7	0.37	Silstone	Grey to brown finely unterbedded siltstone

Table 1: Thermal conductivity of samples at 25°C, and harmonic mean and uncertainty for each specimen

2.4 Discussion and conclusions

For the specimens from Wellington Park-1 and Dutson Downs, there is less than 5% variation form the mean thermal conductivity; this implies that variation in thermal conductivity appears low over the scale of centimetres for these specimens.

The variation in thermal conductivity of specimens measured from the well Sale 13 is significant; up to 70% variation from the mean conductivity (approximately 1.4 W/mK) is shown. Specimens PTR012 (limestone), and PTR014 (coal), are representative of the extremes in variability, showing thermal conductivities of 0.49 W/mK and 2.35 W/mK respectively. This implies that variation of thermal conductivity over the scale of kilometres is significant for the well Sale 13.

Specimen PTR016 showed significant variation in thermal conductivity between its constituent samples, with sample PTR016A showing a variability of 26% from the mean conductivity of 1.70 W/mK. Each sample from specimen PTR016 was re-tested to confirm the results provided on Table 2. Variation of thermal conductivity for this specimen is therefore significant on the scale of centimetres, and should be considered when using this data for the development of geothermal models.

Due to friability, specimens PTR009, PTR011, PTR013, PTR015, and sample PTR014C were prepared via hollow cells. Specimens PTR011 and PTR013, although received in the form of whole core, had a tendency to deteriorate when saturated and were therefore prepared from core placed within hollow cells. Specimens PTR009, PTR015, and PTR014C were received in the form of chips and were inserted into the hollow cells in the form that they were received. Uncertainties of thermal conductivity associated with this preparation method are ± 10%. The following additional points must be considered if extrapolating the results in this report to in situ formations:

- The samples upon which the thermal conductivity measurements were made are only several square centimetres in surface area. While the specimens were chosen to represent the geological sections from which they came, there is no guarantee that the sections themselves are typical of the overall geological formations. This is especially true for heterogeneous formations. This introduces an unquantifiable random error into the results.
- Porosity exerts a primary influence on the thermal conductivity of a rock. Water is substantially less conductive than typical mineral grains6, and water saturated pores act to reduce the bulk thermal conductivity of the rock. Gas-filled pores reduce the bulk conductivity even more dramatically. Results reported in this document are whole-rock measurements. No adjustments were made for porosity. It is to be expected that the thermal conductivity of a given formation will vary from place to place if the porosity of the formation varies (conductivity decreases with increasing porosity).
- Thermal conductivity of rocks is sensitive to temperature, typically decreasing at a rate of around 0.16% per °C. This should be kept in mind when developing models of in situ thermal conductivity.

3. Temperature logging operation and heat flow model

3.1 Introduction

Hot Dry Rocks Pty Ltd (HDRPL) was commissioned by Petratherm Ltd (PTR) to undertake temperature logging and heat flow modelling of the Sale 13 groundwater bore in the Gippsland Basin, Victoria.

Sale 13 was drilled during June–July 1975 to a depth of 1,049.8 mGL, and has until recently acted as a groundwater observation bore as part of the Victorian Government's State Observation Borehole Network. Sale 13 is located on the western shoreline of Lake Wellington, east of the township of Sale. Sale 13 is within Greenearth Energy Limited's GEP12 (Geothermal Exploration Permit) license, some 800m west of Petratherm's GEP24 license.

3.2 Temperature logging

An operation plan was submitted to DPI on the 8th of May 2009 and accepted on the 18th of June 2009. The operation was safely conducted on the 23rd and 24th of June. Sale 00013, located on Greenearth's GEP 12 was still opened to at least 950m and the probe successfully recorded a bottom of hole temperature of 67.2°C at 950m.

3.3 Heat flow

Heat flow is a power unit expressed at surface (mW/m2) and is a function of heat generated within the crust plus heat conducted from the mantle.

The principle aim of geothermal exploration is to locate anomalously high temperatures within a productive reservoir at an economically and technically viable drilling depth. The thermal state of a region is usually expressed at the surface in the form of heat flow units (mW/m2) and it is generally assumed that heat is transported to the surface by conductive means.

In a conductive heat regime the temperature T, at depth z is equal to the surface temperature T0 plus the product of heat flow Q and thermal resistance R, such that:

T=T0+QR, where R=z/(average thermal conductivity between the surface and z).

Consequently the most highly prospective regions for geothermal exploration are those that have geological units of sufficiently low conductivity (high thermal resistance) in the cover sequence combined with high heat flow. Heat flow is a product of temperature gradient and rock thermal conductivity and is therefore not directly measured. The measurement of heat flow is a precision skill that requires a detailed understanding of physical conditions in the bore and the physical properties of the rocks; including potential advective processes that may influence bore temperature (such as ground water flow) and the temperature dependence of conductivity.

HDRPL utilises its own 1D Heat Flow Modelling Software to determine heat flow from measured values. Forward modelled temperature distribution with depth, incorporating advective influences and temperature dependence of thermal conductivity, is compared against the observed temperature profile within a bore. The precise vertical heat flow value is determined that best fits the observed

profile. The results of 1D heat flow modelling should be treated with caution when extrapolating over lateral distances, because heat refraction can lead to significant variation in vertical heat flow over relatively short lateral distances. Detailed 2D or 3D modelling is recommended if such effects are suspected.

3.4 Results

The heat flow model for Sale 13 (Figure 1) illustrates an excellent fit between the observed and predicted temperature profiles. The well intersected a sandstone/ marl/limestone sequence in the upper approximately 846 m (thermal conductivities ranged from 1.21–2.35 W/mK) and bottomed within a coal/carbonaceous siltstone unit (thermal conductivities ranged from 0.49–1.70 W/mK)1. The conductive surface **heat flow** is **75.0±3.1mW/m²**.

The deep coaly interval displays very low thermal conductivity values. As a result, no temperature correction has been applied in this particular 1D heat flow model since generic empirical published temperature correction formulae are not calibrated for very low conductivity measurements as seen in this well.

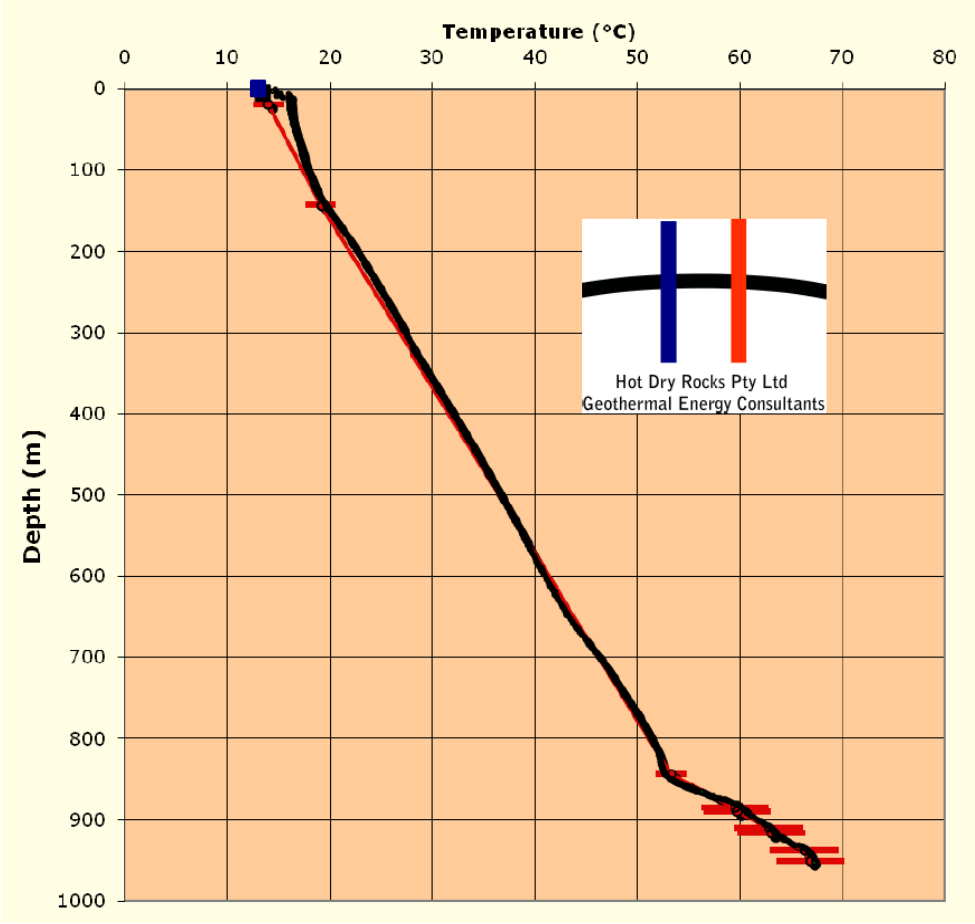

Figure 1: Sale 13 groundwater bore. Red line is the modelled temperature profile for the stated heat flow and measured rock thermal conductivity data. Black line is the measured precision temperature log.

4. Core analysis

4.1 Introduction

This section presents the results of a routine core analysis study performed on the sample PTR-1, a piece of core collected at the core library from the well Megascolides-1 at 1903m. A core plug was taken from

the core piece and porosity and permeability measurements were performed by Weatherford laboratories, Brisbane.

4.2 Methodology

4.2.1 Sample preparation

One core plug of 1" diameter was drilled from the piece of core using synthetic brine as the coolant. The sample was then trimmed to maximum length using a diamond impregnated blade.

4.2.2 Cleaning and drying

Cleaning was performed in a modified soxhlet system (Appendix I) using a 3:1 chloroform/methanol azeotrope. Cleaning continued until tests for oil (fluorescence under UV lights) and salt (silver nitrate precipitation) showed negative. The clean sample was dried to constant weight in a humidity oven at 60°C and 40% relative humidity. Once dry, the sample was cooled to room temperature in an airtight chamber.

4.2.3 Porosity

The clean and dry plug was sealed in a matrix cup and a known volume of helium at 100 psi reference pressure was introduced to the cup. From the resultant pressure, the unknown volume, i.e. the grain volume, was calculated using Boyles Law. The bulk volume of each plug was determined by Archimedes' Principal. The difference between the grain volume and the bulk volume is the pore volume. The porosity is calculated as the volume percentage of pore space with respect to the bulk volume.

$$P_1 V_1 = P_2 V_2$$

$$\Rightarrow \quad P_1 V_r = P_2 (V_r + V_c - V_g)$$

$$V_p = V_b - V_g$$

$$\text{Ambient Porosity \%} = V_p / V_b * 100\%$$

Where

- P_1 = initial pressure (psig)
- P_2 = final pressure (psig)
- V_r = reference cell volume (cm^3)
- V_c = matrix cup volume (cm^3)
- V_g = grain volume (cm^3)
- V_p = pore volume (cm^3)
- V_b = bulk volume (cm^3)

The porosity (and permeability) at simulated overburden stress was measured by mounting the sample into a thick walled rubber sleeve and then loading the assembly into a hydrostatic cell. With an 'ambient' confining stress of 400 psi applied to the sample, helium held at 100 psi reference pressure was released into the samples pore space. The new pressure was then recorded. The confining stress was then increased to overburden pressure and the pore pressure noted at equilibrium. The changes in pore pressure, together with the previously determined parameters in the ambient analyses, allowed the calculation of porosity at overburden conditions, as follows:

$$\text{Overburden Porosity \%} = (V_p - \delta V_p)/(V_b - \delta V_b) * 100\%$$

4.2.4 Permeability to air

The sample was placed into a hydrostatic cell and the confining pressure was then increased to 4950 psi overburden pressure. In order to determine permeability, a known air pressure was applied to the upstream face of the sample, creating a flow of air through the core plug. Air permeability for the core sample was calculated using Darcy's Law through knowledge of the upstream pressure, flow rate, viscosity of air and sample dimensions.

$$Ka = (2000BP.\mu.q.L)/(P_1^2-P_2^2).A$$

Where

Ka	=	*air permeability (milliDarcy's)*
BP	=	*barometric pressure (atmospheres)*
μ	=	*gas viscosity (cP)*
q	=	*flow rate (cm^3/s) at barometric pressure*
L	=	*sample length (cm)*
P1	=	*upstream pressure (atmospheres)*
P2	=	*downstream pressure (atmospheres)*
A	=	*sample cross sectional area (cm^2)*

4.2.5 Grain density

The apparent grain density is calculated by dividing the weight of the plug by the grain volume, determined from the helium injection porosity measurement.

$$P = Wt/Vg$$

Where

ρ	=	*grain density (g/cm^3)*
Wt	=	*weight of sample (g)*
Vg	=	*grain volume (cm^3)*

4.3 Results

Sample	Depth m	Overburden pressure (psi)	Overburden Porosity Helium %	Grain Density (g/cm^3)	Overburden Permeability to Air (mD)
PTR-1	1903	4950	2.3	2.72	0.001

5. Petrographic description

5.1 Introduction

A thin section was prepared from the core plud drilled in PTR-1. The plug PTR-1 (Megascolides-1-1903m), with accompanying thin section was sent to Mason Geoscience Pty Ltd for a routine petrographic description.

5.2 Methodology

Conventional transmitted polarised light microscopy was used to prepare the routine petrographic description. Paragenetic stages of development of the rock are indicated in the mineral modal list, where each mineral is assigned to a numerical paragenesis (paragenesis 1 is earliest; paragenesis 2 overprints 1; paragenesis 3 overprints both 2 and 1; etc). The paragenetic stages display relative timing insofar as they can be determined.

A photomicrograph is included with the description to illustrate the principal textural and mineralogical features of the rock.

5.3 Petrographic description

5.3.1 Hand specimen

The drill core plug represents a uniformly fine-grained pale greenish grey rock in which layering is defined by minor thin wispy dark subparallel laminae. The sample bubbles strongly in reaction with dilute HCl, suggesting calcite occurs throughout the rock.

5.3.2 Rock name

Calc-sandstone

5.3.3 Petrography

A visual estimate of the modal mineral abundances gives the following:

Mineral	Vol%	Origin
Quartz	72	Clastic grains 1
Lithics (meta-?siltstone)	3	Clastic grains 1
Feldspar (mainly K-feldspar)	2	Clastic grains 1
Opaques/leucoxene	1	Clastic grains 1 (altered ?ilmenite)
Garnet	<1	Clastic grains 1
Muscovite	Tr	Clastic grains 1
Tourmaline	Tr	Clastic grains 1
Zircon	Tr	Clastic grains 1
Rutile	Tr	Clastic grains 1
Clay (pale brown, ?smectite)	10	Diagenetic/very low-grade metamorphic 2
Carbonate (calcite)	10	Diagenetic/very low-grade metamorphic 2

In thin section, this sample displays a well-preserved framework-supported clastic sedimentary texture, modified by incipient recrystallisation and grain suturing of diagenetic to low-grade metamorphic origin.

Clastic particles are abundant, most with sizes in a fine sand particle size range of 100-150µm (0.10-0.15mm). Rare larger grains ~0.4-0.8mm in size are very irregularly scattered through the rock. Quartz is abundant, forming angular grains that are firmly sutured where in contact. Small lithic fragments occur in minor amount, and appear to be meta-siltstones composed of fine-grained assemblages of quartz and

muscovite. Feldspar grains are similar in size and shape to quartz, but display their lower birefringence and cleavage. Opaque grains display turbid dark brown alteration effects, and may represent leucoxene (ie cryptocrystalline Ti-mineral) after ilmenite. Garnet is present in minor amount, displaying the characteristic optical properties of this mineral (colourless, high relief, fractured but not cleaved, perfectly isotropic under crossed polarisers). Muscovite forms uncommon flakes. Tourmaline occurs as small subrounded grains that display varied pleochroism: some are orange-brown and others are pale green. Zircon (colourless, high relief, high birefringence) forms small subrounded grains and less common euhedral terminated prisms, suggesting varied zircon populations are present. Rutile occurs as uncommon small deep yellow grains. Indistinct layering is defined by minor thin heavy mineral laminae in which grains of opaques/leucoxene (ie altered ilmenite), garnet, and zircon are more abundant than elsewhere.

Clay occurs as pale brown material that forms very fine-grained angular patches between the clastic grains, and in places forms discontinuous rims around some clastic grains. Its pale brown colour suggests it may be ?smectite, but positive identification would require additional analysis (eg X-ray diffraction). Carbonate (calcite) occurs in significant amount as anhedral grains located between the clastic particles. The calcite is more-or-less uniformly distributed through the rock, and commonly occurs in close association with the clay patches in interparticle pores.

5.3.4 Interpretation

This sample formed as a fine-grained sandy clastic sediment composed of abundant closely-packed crystal fragments (quartz >> feldspar, opaques/leucoxene, garnet, muscovite, tourmaline, zircon, rutile) and minor lithic fragments (meta-siltstone) accompanied by a moderate proportion of fine interparticle matrix (clay = carbonate). Primary layering was defined by minor thin heavy mineral laminae containing higher abundances of opaques/leucoxene, garnet and zircon. A shallow marine environment is inferred from the heavy mineral lamination and the presence of carbonate which most likely formed as a chemical sedimentary component in the primary matrix.

Following deposition and burial, the sandy materials suffered mild diagenetic or very low-grade metamorphic effects. This resulted in firm suturing of the clastic grains, and caused recrystallisation of the clay and carbonate components in the matrix.

Figure 2: Megascolides-1-1903m (Transmitted light, crossed polarisers, Obj. x20, Image P9014978). This view of calc-sandstone illustrates the abundant well-sorted clastic quartz grains (white to grey) with interparticle pores lined by clay (turbid dull brown colour) and filled by recrystallised carbonate calcite, high pastel coloured grains).

Appendix1 – List of contractor commissioned

Data	Contractor	Address
Thermal conductivity	Hot Dry Rock Pty Ltd	PO Box 251 South Yarra, Vic 3141
Temperature logging	Hot Dry Rock Pty Ltd	PO Box 251 South Yarra, Vic 3141
Routine core analysis, porosity/permeability	Weatherford laboratories	8 Cox Road, Windsor Qld 4030
Petrographic description	Mason Geoscience Pty Ltd	141 Yarrabee Rd Greenhill, SA, 5140